HUMAN VACCINES & IMMUNOTHERAPEUTICS
2018, VOL. 14, NO. 11, 2786–2801
https://doi.org/10.1080/21645515.2018.1489192

Taylor & Francis
Taylor & Francis Group

RESEARCH PAPER

Specific T cell induction using iron oxide based nanoparticles as subunit vaccine adjuvant

Lázaro Moreira Marques Neto [a], Nicholas Zufelato[b], Ailton Antônio de Sousa-Júnior [b], Monalisa Martins Trentini[a], Adeliane Castro da Costa[a], Andris Figueiroa Bakuzis[b], André Kipnis [a], and Ana Paula Junqueira-Kipnis[a]

[a]Instituto de Patologia Tropical e Saúde Pública, Universidade Federal de Goiás (IPTSP-UFG), Brasil; [b]Instituto de Física, Universidade Federal de Goiás (IF-UFG), Brasil

ABSTRACT

Metal-based nanoparticles (NPs) stimulate innate immunity; however, they have never been demonstrated to be capable of aiding the generation of specific cellular immune responses. Therefore, our objective was to evaluate whether iron oxide-based NPs have adjuvant properties in generating cellular Th1, Th17 and TCD8 (Tc1) immune responses. For this purpose, a fusion protein (CMX) composed of *Mycobacterium tuberculosis* antigens was used as a subunit vaccine. Citrate-coated $MnFe_2O_4$ NPs were synthesized by co-precipitation and evaluated by transmission electron microscopy. The vaccine was formulated by homogenizing NPs with the recombinant protein, and protein corona formation was determined by dynamic light scattering and field-emission scanning electron microscopy. The vaccine was evaluated for the best immunization route and strategy using subcutaneous and intranasal routes with 21-day intervals between immunizations. When administered subcutaneously, the vaccine generated specific $CD4^+IFN\text{-}\gamma^+$ (Th1) and $CD8^+IFN\text{-}\gamma^+$ responses. Intranasal vaccination induced specific Th1, Th17 ($CD4^+IL\text{-}17^+$) and Tc1 responses, mainly in the lungs. Finally, a mixed vaccination strategy (2 subcutaneous injections followed by one intranasal vaccination) induced a Th1 (in the spleen and lungs) and splenic Tc1 response but was not capable of inducing a Th17 response in the lungs. This study shows for the first time a subunit vaccine with iron oxide based NPs as an adjuvant that generated cellular immune responses (Th1, Th17 and TCD8), thereby exhibiting good adjuvant qualities. Additionally, the immune response generated by the subcutaneous administration of the vaccine diminished the bacterial load of Mtb challenged animals, showing the potential for further improvement as a vaccine against tuberculosis.

ARTICLE HISTORY
Received 26 March 2018
Accepted 12 June 2018

KEYWORDS
Infectious disease; Manganese ferrite; antigenicity; Th1; Th17 TCD8 cells

Introduction

Adjuvants are substances that enhance and extend the immune response generated against a co-administered antigen. Only a few adjuvants are licensed for use in human vaccines, and even fewer efficiently induce a cellular immune response. This type of response is required for protection against some diseases that are of concern around the world, such as tuberculosis (TB) and malaria.[1] Therefore, the discovery of new vaccine adjuvants is the main goal of vaccinology. In a vaccine formulation, together with the adjuvant, the antigen guides the adaptive immune response toward the target microorganism and is associated with the long-lasting (memory) response.[2] However, there is evidence indicating that proteins from microorganisms are recognized not only by major histocompatibility complex (MHC) II/T cell receptors (TCRs) but also by the innate immune response via some pattern recognition receptors (PRRs), such as Toll-like receptors (TLRs).[3,4] Hence, the immunization route and the vaccination dose also impact generation of the immune response, especially the protective mucosal immune response.[5,6]

Magnetic nanoparticles (MNPs) have several applications in nanomedicine such as contrast agents in magnetic resonance imaging (MRI), magnetic tracers in magnetic particle imaging (MPI) and alternating current biosusceptometry (ACB), and in magnetic hyperthermia therapy.[7-10] For a long time, nanoparticles (NPs) were only considered to be delivery systems in vaccines; however, there is now evidence showing that NPs can act as vaccine adjuvants with immunostimulatory capabilities.[11] Nonetheless, the use of metallic NPs in vaccinology is rare, and many effects and mechanisms of NPs have yet to be elucidated.[12] Some of the most common nanoparticles are iron oxide ones: magnetite – Fe_3O_4 – that consist of a cubic ferrite spinel structure containing one $1Fe^{2+}$; $2Fe^{3+}$; $4O^{2-}$ in the molecular structure. This type of NP has been utilized as a vaccine platform against malaria only by Pusic et al. (2013), who demonstrated that vaccination with IONPs induces higher titers of parasite-inhibitory antibodies than vaccination with ISA51 (montanide) as an adjuvant. It was also demonstrated that IONPs activated dendritic cells (DCs) *in vitro* and enhanced CD86 expression. In addition, IONPs enhanced IL-6, TNF-α, IL-1β, IFN-γ, and IL-12 production, which correlated with the Th1 (IL-12) and Th17 (IL-6 and IL-1β) responses.[13]

In 2015, TB became the world's leading cause of infectious disease-related death, surpassing acquired immune deficiency

CONTACT Ana Paula Junqueira-Kipnis apkipnis@gmail.com Instituto de Patologia Tropical e Saúde Pública, Universidade Federal de Goiás, Rua 235 esquina com Primeira Avenida. Setor Universitário. Goiânia, Goiás, 74605-450, Brazil.

Supplemental data for this article can be accessed on at tandfonline.com/khvi.

syndrome (AIDS). It is estimated that one-third of the global population is infected with this bacillus, and the development of an effective vaccine to prevent disease activation and new infections is very important for TB eradication.[14] Although it is widely accepted that balanced Th1 and Th17 cellular responses correlate with protection against infection, TB is a complex disease whose pathogenesis reflects the interactions between *Mycobacterium tuberculosis* (*Mtb*) and the host immune system, which are not fully understood.[15] Thus, TB represents a model disease for evaluating the adjuvant properties of IONPs in eliciting cellular immune responses.

CMX protein is a fusion protein composed of portions of immunodominant antigens of *Mtb*: one is a peptide from Ag85c, a mycolyl-transferase protein responsible for the synthesis of *Mtb* cell-wall lipids[16]; another is a peptide from MPT51, a homolog of the Ag85 family but with functions associated with cell adhesion and virulence[17,18]; and the third is the entire HspX protein, a heat shock protein associated with the latent phase of mycobacterial infection.[19,20] CMX has been used in several vaccination strategies; this protein is capable of generating a Th1 response (together with CpG/DNA) in a subunit vaccine formulation[21] and of producing Th1 and Th17 responses to protect against TB when expressed in live vectors (*Mycobacterium smegmatis* or *M. bovis* bacille Calmette-Guerin (BCG).[22-24] Recently, it was shown by da Costa and colleagues that CMX protein alone could influence the innate immune response and exhibit immunomodulatory activity, which was partially TLR-4 and TLR-2 dependent, inducing NF-κB, IL-6, TGF-β and IL-1β expression in bone marrow-derived macrophages.[25]

The complete pathway driving T cell responses in the respiratory tract (targeted by TB) is still unclear. However, there is evidence that intranasal vaccination can stimulate DCs responsible for generating T cells and recruiting them back to the lungs through the induction of CCR4 expression.[26] BCG is a globally accepted TB vaccine used in humans and is administered subcutaneously (SC) but does not provide long-term protection. Animals, such as guinea pigs, mice and macaques, are currently used as models for investigating new vaccines against TB. BCG vaccine administered SC is most frequently used as a control; however, the use of BCG or other vaccines (viral vectors or subunit vaccines) via the intranasal route can improve the immune response (Th1), change the response profile in the lungs, increase the mucosal Th17 response, and enhance the protection against aerosol challenges.[27-29]

The objective of this work was to evaluate the adjuvant properties of manganese ferrite ($MnFe_2O_4$)-NPs in the context of a nanoparticulate subunit vaccine composed of CMX fusion protein adsorbed on it toward the generation of specific Th1 (CD4 T lymphocyte, IFN-γ producer), Th17 (CD4 T lymphocyte, IL-17 producer) and Tc1 (CD8 T lymphocyte, IFN-γ producer) responses.

Results

NP vaccine characterization

The CMX protein, with a molecular mass of approximately 36 kDa, was used to cover the citrate-coated $MnFe_2O_4$ NPs to form NCMX. The size of the citrate-coated $MnFe_2O_4$ NPs obtained by transmission electron microscopy (TEM) was 15.4 $\pm$ 4.6 nm (Fig. 1B). However, when dispersed in liquid, attractive intraparticle interactions, mainly van der Waals and magnetic interactions, led to the formation of agglomerates. This result was confirmed by the larger mean hydrodynamic diameter (86 nm) observed by dynamic light scattering (DLS) prior to protein coating (Fig. 1A, upper curve). Indeed, DLS also indicated that the CMX protein adsorbed onto the NPs by affinity, as demonstrated by observation of a larger nano-compound with a mean hydrodynamic diameter of approximately 622 nm (Fig. 1A, bottom curve). Protein adsorption was also confirmed by field-emission scanning electron microscopy (FE-SEM) analysis. The uncoated $MnFe_2O_4$ NPs, namely Nano, those not coated with CMX, were 151 $\pm$ 25 nm in size (Fig. 1C). In contrast, the formation of the CMX corona in the NCMX nanostructure yielded particles with an increased size of 881 $\pm$ 130 nm (Fig. 1D). The larger value measured by FE-SEM than by DLS was expected; in DLS, the particle size was measured in the liquid media, while in FE-SEM, the sample was dried. Therefore, one expects part of the protein corona to disconnect from the nanostructure, resulting in a larger size. The attachment of CMX to the NPs was also confirmed by immunodot blot assays using anti-CMX antibodies (Fig. 1E). As shown, the majority of the protein used was coated onto the $MnFe_2O_4$ NPs, and only a residual quantity of the protein remained in the supernatant after magnetic lateral separation (fourth dot of Fig. 1E). To verify the amount of CMX linked to the nanostructure, the protein was separated by the addition of sodium dodecyl sulfate (SDS) and centrifuged; then, the supernatant was utilized for western blotting (compared to a known CMX concentration). By doing so, it was possible to determine that the concentration of CMX protein attached to the NP was very close to the total concentration used to cover the NP, i.e., a final concentration of 200 μg/mL (Fig. 1F).

Subcutaneous NCMX vaccination induces Th1 and Tc1 responses and an increase in the number of lymphatic endothelial cells (LECs) ($gp38^+CD31^+$ cells)

To determine whether the vaccine formulated with NPs was immunogenic, mice were vaccinated SC three times at 21-day intervals. To optimize the dose necessary to induce specific immune responses, two concentrations of NPs were used, 10 μg (SC10) and 50 μg (SC50), which were formulated with 20 μg of CMX. Twenty-one days after the last immunization, the specific immune responses in the spleen and lungs were evaluated (Fig. 2A). T $CD4^+$ lymphocytes expressing IFN-γ (Th1), T $CD4^+$ lymphocytes expressing IL-17 (Th17), and T $CD8^+$ lymphocytes expressing IFN-γ (Tc1) were analyzed by flow cytometry. Both formulations demonstrated the capacity to generate Th1 (Fig. 2B and 2C) and Tc1 (Fig. 2F and 2G) responses in the spleen and lungs of vaccinated mice. None of the groups showed a Th17 response (Fig. 2D and 2E) using this route with these tested doses. The generated CMX-specific humoral response varied among the groups; subcutaneous vaccination using 50 μg of NPs presented the highest IgG1 and IgG2a levels. However, the level of IgG2a to IgG1 was balanced for both vaccine formulations (Fig. 2H and I).

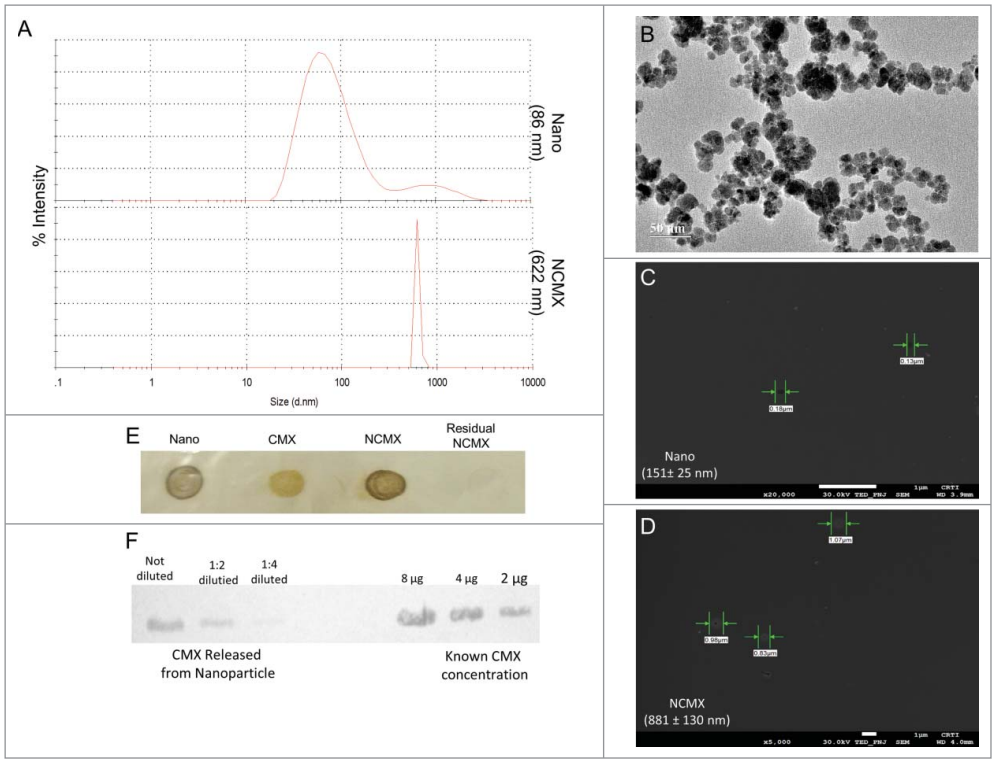

Figure 1. Construction and characterization of $MnFe_2O_4$ NPs coated with CMX. (A) DLS results of citrate-coated $MnFe_2O_4$ NPs (Nano, upper panel) and citrate-coated $MnFe_2O_4$ NPs incubated with CMX (NCMX, lower panel). (B) TEM images of citrate-coated $MnFe_2O_4$ NPs. Characterization of CMX protein corona formation of Nano (C) and NCMX (D). (E) NCMX samples were separated by lateral magnetic separation and utilized for the dot plot. The first dot represents only citrate-coated Nano; the second dot represents only CMX as a positive control; the third dot represents magnetically separated citrate-coated Nano covered with CMX (NCMX); and the last dot is the residual protein in the supernatant after the adsorption of CMX onto the NPs (residual CMX). (F) Quantification of CMX adsorbed onto the NPs. NCMX was incubated with 10% SDS and then centrifuged, and the supernatant left was used for western blotting and comparison with a known concentration of CMX.

LECs have been shown to proliferate, store antigens in the lymph nodes, and support the maintenance of T $CD8^+$ memory cells under proinflammatory conditions. Thus, since the subcutaneous route induced a robust Tc1 response in the spleen, the capacity of NCMX to induce LEC ($gp38^+CD31^+$) proliferation was evaluated. Evaluation of the axillaries lymph nodes 4 days after subcutaneous vaccination showed that NCMX induced an increase in the level of LECs, while none the CMX protein or Nano alone was able to induce this proliferation (Fig. 3).

Subcutaneous vaccination followed by intranasal boost generates specific Th1 and Tc1 lymphocytes but does not induce Th17 cells

Although both vaccine formulations were immunogenic, an important component of the supposed protective immune response against *Mtb* was missing. Th17 cells, when stimulated together with Th1 cells, are known to aid the generation of a better protective response.[30,31] The combination of subcutaneous and intranasal mucosal vaccination has been shown to generate Th17 cells.[32,33] Thus, it was hypothesized that in order to generate specific Th1/Tc1/Th17 responses, a combination immunization route should be used. The mixed vaccination scheme generated specific Th1 (Fig. 4A) cells in the spleen and lungs (Fig. 4B) of immunized mice. Additionally, specific Tc1 cells (Fig. 4E) were induced in the spleen. However, no Th17-specific response was observed in the spleen (Fig. 4C) or lungs (Fig. 4D) of vaccinated mice. The nanoparticle alone was also used as control, however as we evaluated the specific response to CMX, no response elicited (Supplementary Fig. 5). The humoral response elicited by this vaccination strategy was weaker than that generated by subcutaneous vaccination, and the intranasal booster led to little improvement in the antibody response (Fig. 4G and H). In summary, the results show that the NCMX formulation efficiently induces Th1 and Tc1 responses but not a Th17 response when the subcutaneous and intranasal routes are used.

Intranasal instillation can stimulate Th17 in addition to Th1 and Tc1 responses in the lungs

Since specific Th17 cells were not generated in the lungs when intranasal vaccination was used as a booster, a vaccination strategy using only intranasal vaccination (a mucosal immune stimulator) was used (Fig. 5A). The vaccination stimulated specific Th1 (Fig. 5B) and Tc1 (Fig. 5D) responses in the lungs as well as the important Th17 (Fig. 5C) response; however, no antibody responses were observed (Fig. 5E and F).

Multiple exposures of the lung parenchyma to inorganic NPs, especially iron and manganese NPs, could result in lung damage. Although the animals did not present any sign of stress or disease (data not shown), the morphology and histology of the lung tissue were evaluated. Mice vaccinated with the $MnFe_2O_4$ NP and NCMX formulations exhibited increased lung cellularity without the formation of

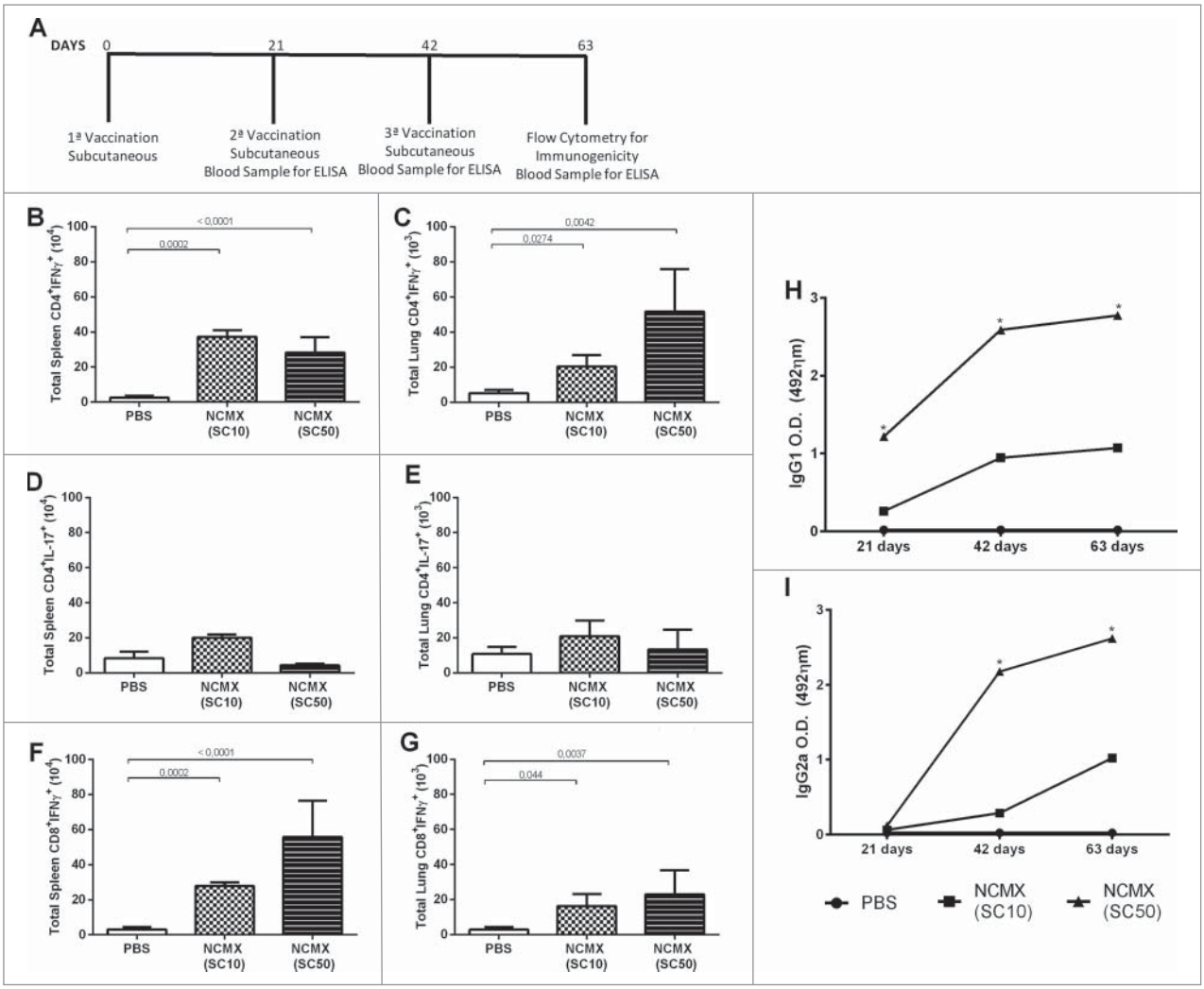

Figure 2. Immune response to subcutaneous vaccination is not affected by the NP dose in the formulation. Groups of four mice were immunized SC two times with 100 μL of NCMX, and the third booster was administered via intranasal instillation. Twenty-one days after the last immunization, the spleen and lungs were collected and analyzed by flow cytometry for Th1, Th17, and Tc1 lymphocytes (A).-one days after the last immunization, the spleen and lungs were collected and analyzed by flow cytometry for Th1, Th17, and Tc1 lymphocytes (A). The number of Th1 (CD4+IFN-γ+), Th17 (CD4+IL-17+), and Tc1 (CD8+IFN-γ+) cells in the spleen (B, D and F, respectively) and lungs (C, E and G, respectively) are shown. Differences between the means of the groups were determined by ANOVA and post-hoc test, and p values are shown. Serum samples were collected, and the humoral immune response was evaluated by measuring the levels of IgG1 (H) and IgG2a (I). Differences between the means of the groups were determined by ANOVA and significant differences with $p < 0.05$ are shown with an asterisk (*).

arteriolar cuffs, which is indicative of cell migration. However, the $MnFe_2O_4$ NPs resulted in a lower cellularity index, and this difference could be correlated with particle size and aggregation (Fig. 6).

The hemolytic effect of the $MnFe_2O_4$ NPs (10 μg, 50 μg, 100 μg and 500 μg) and NCMX (with 20 μg of CMX and 10 μg, 50 μg, 100 μg and 500 μg of $MnFe_2O_4$ NPs) is demonstrated in Supplementary Fig. 3. Hemolysis increased slightly with the increasing tested concentrations; however, hemolysis did not exceed 20% for any sample, even with the highest concentration tested being 10-fold greater than the vaccine concentration. Additionally, twenty-one days after two intranasal vaccinations, two subcutaneous and three subcutaneous vaccinations (using 10 μg of $MnFe_2O_4$ NPs and 20 μg of CMX), the heart, kidneys and liver were collected, sectioned, stained with hematoxylin and eosin (H&E) and evaluated for signs of chronic toxicity or persistent organ damage. No disturbances or injuries were found in any of these organs (Supplementary Fig. 4).

CMX-specific Th1 and Tc1 recall responses after Mtb *challenge cause reduction in the bacterial load*

Because the subcutaneous and the combined subcutaneous and intranasal vaccination strategies induced cellular immune responses, vaccinated mice were challenged with Mtb to determine whether the response could be recalled. The Mtb challenge resulted in increased numbers of specific Th1 cells in the lungs of all infected groups. However, the greatest increase in $CD4^+IFN\text{-}\gamma^+$ cells was observed in animals SC vaccinated with NCMX (Fig. 7B-D). Additionally, the *Mtb* infection induced an increase in the CMX-specific Tc1 population. Vaccination with NCMX recalled the CMX-specific Tc1 population (doubled the amount observed for *Mtb*-challenged or BCG-vaccinated animals) to the lungs of the vaccinated mice (Fig. 7C-E).

Preservation of the lung architecture (healthy/saline control; Fig. 8A) is an essential feature of vaccines against TB. The lungs of the *Mtb*-infected group exhibited expressive lymphocytic and neutrophilic infiltrates, compromising the entire lung

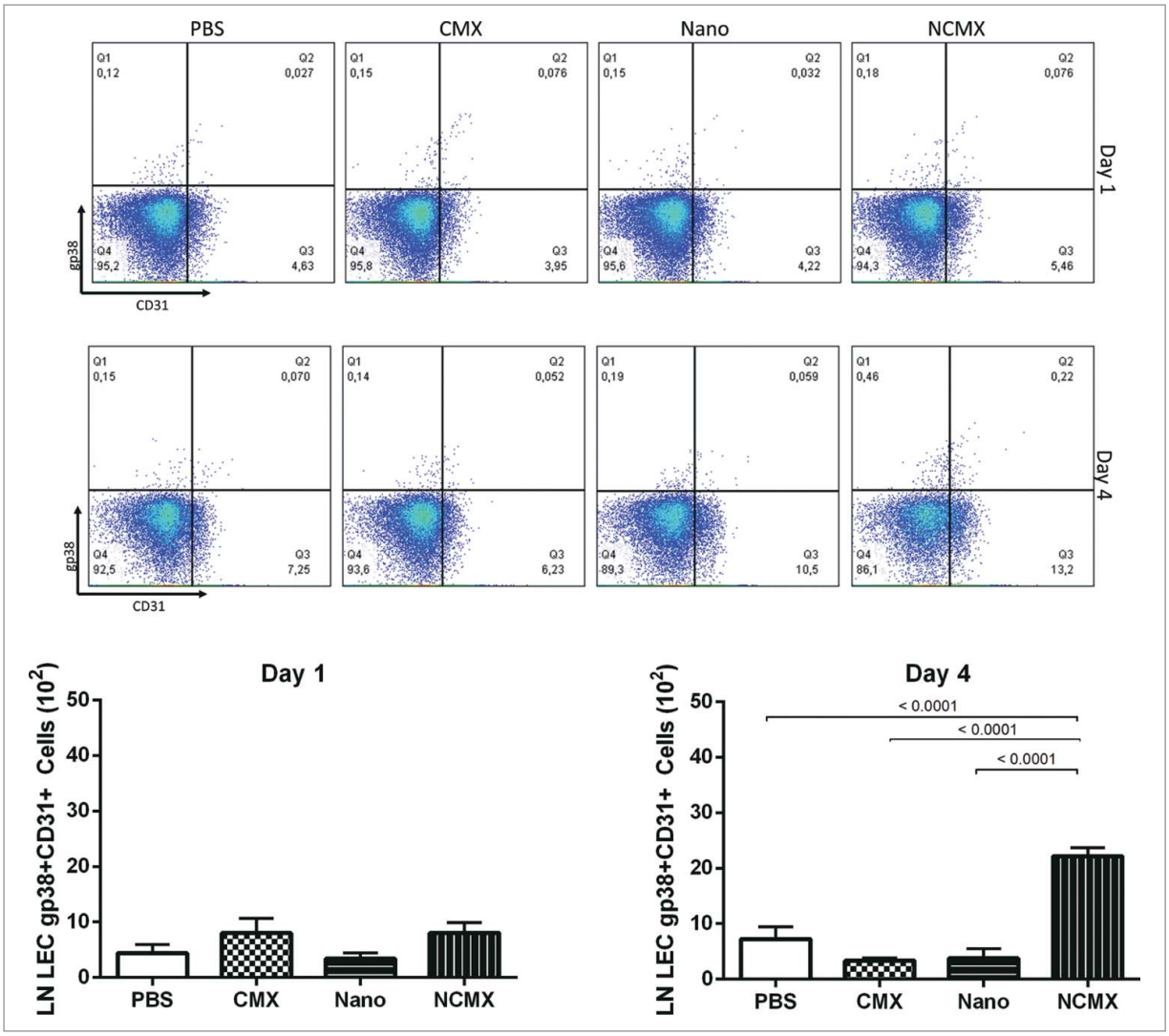

Figure 3. Subcutaneous immunization induces an increase in LECs ($gp38^{+}CD31^{+}$) in draining lymph nodes. Representative dot plots for each group are shown above the graphs of lymph node endothelial cell counts evaluated based on CD31, gp38 and CD21/35 staining 1 day (left graph) or 4 days (right graph) after immunization with CMX or Nano only or with the NCMX formulation. Differences among groups were determined by one-way ANOVA, and p values are shown. Significant differences were found among the groups, n = 4 mice.

tissue architecture, together with the presence of foamy macrophages (Fig. 8B). On the other hand, BCG-vaccinated mice showed fewer lung lesions, preserving the alveolar spaces, and limited lymphocytic tissue infiltration (Fig. 8C). However, while the subcutaneous NCMX vaccination preserved the lung architecture but with areas of mononuclear inflammatory cell infiltration (Fig. 8D), the mixed (subcutaneous and intranasal) NCMX vaccination showed larger areas of mononuclear inflammatory cell infiltration that compromised the alveolar structure (Fig. 8E).

Finally, diminishing the bacterial burden in the lungs of infected hosts is one of the main goals of *Mtb* vaccines. Thus, we assessed whether vaccination with NCMX could generate a response that could protect mice against intravenous Mtb challenge. NCMX vaccination reduced the number of bacteria recovered from the lungs of challenged mice by half log unit compared with the number of bacteria recovered from the lungs of unvaccinated mice (saline control), while BCG vaccination reduced the number of bacteria by approximately 0.8 log unit (Fig. 8F).

Discussion

The search for new adjuvants is one of the main goals of vaccinology. NPs have been reported in several studies as being able to interact with the immune system and have been demonstrated to serve as adjuvants capable of inducing a humoral immune response. The capacity of NPs to induce T cell responses is still unclear. Consequently, cellular (Th1 and Th17) immune responses, even when antigens are coupled with NPs, are correlated with the utilization of TLR adjuvants or other potent adjuvants.[12,34] In this work, we presented a new NP adjuvant for a subunit vaccine, which we tested in a murine model of TB. The adjuvant used a fusion protein named CMX, which is a protein composed of three *Mtb* antigens that has previously been shown to induce a protective response against TB in several vaccine formulations.[22-24] The NCMX vaccine was tested using subcutaneous and intranasal vaccination schemes. All strategies showed the ability to induce a specific immune response to CMX, and when the vaccine was administered SC followed by challenge with *Mtb*, CMX-specific Th1

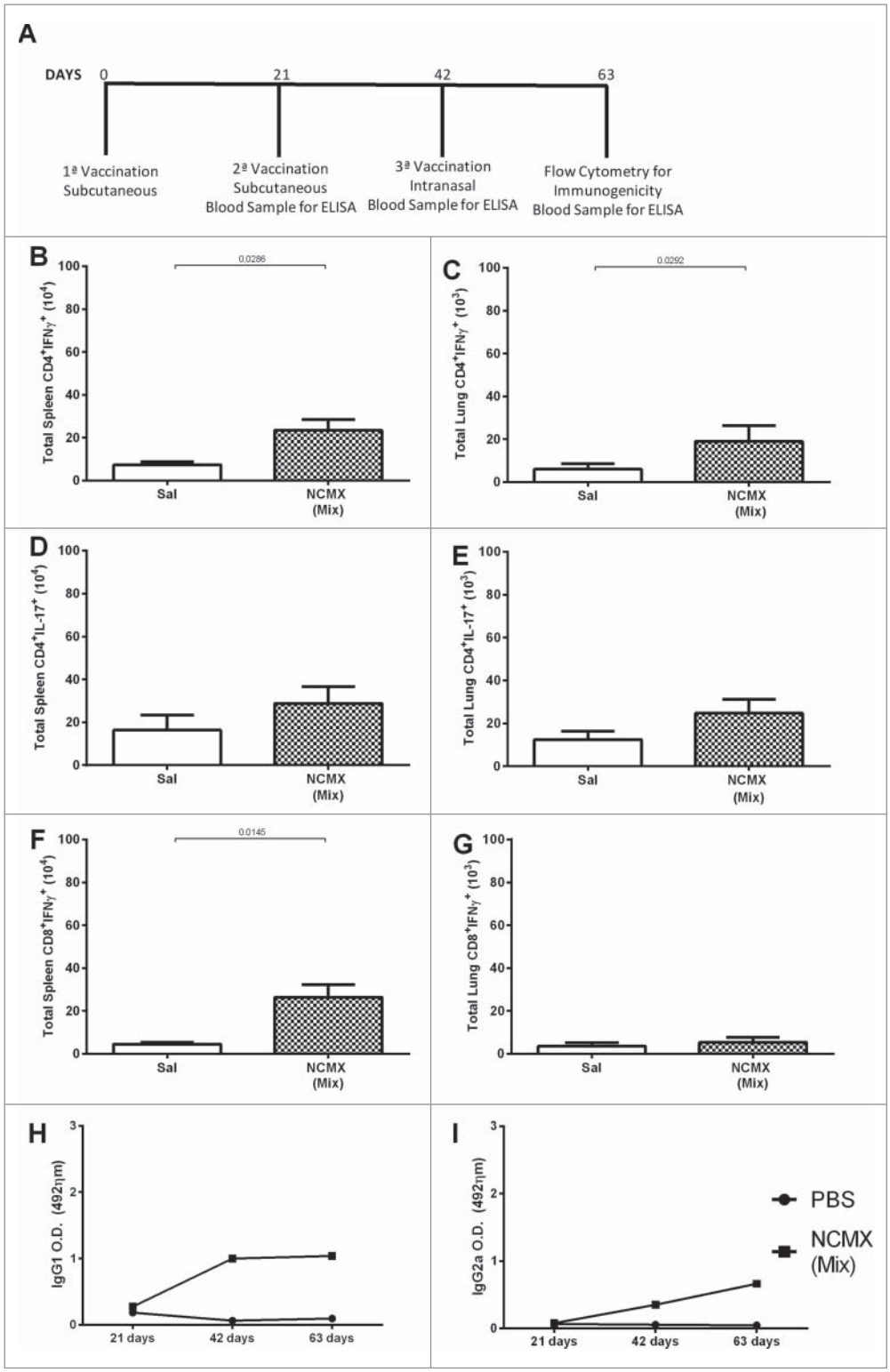

Figure 4. Mixed vaccination induces weak lung Th1 and splenic Th1 and Tc1 responses. Mice were immunized SC two times with 100 μL of NCMX, and the third booster was administered via intranasal instillation. Twenty-one days after the last immunization, the spleen and lungs were collected and analyzed by flow cytometry for Th1, Th17, and Tc1 lymphocytes (A). The number of Th1 ($CD4^+IFN\text{-}\gamma^+$), Th17 ($CD4^+IL\text{-}17^+$), and Tc1 ($CD8^+IFN\text{-}\gamma^+$) cells in the spleen (B, D and F, respectively) and lungs (C, E and G, respectively) are shown. Serum samples were collected, and the humoral immune response was evaluated by measuring the levels of IgG1 (H) and IgG2a (I). Differences between the means of the groups were determined by Student's *t*-test, and p values are shown. Significant differences were found between the groups, n = 4.

and Tc1 responses were achieved and conferred half log protection against TB.

The NPs used here is very similar to magnetite, but instead of containing Fe^{2+} in this structure it has Mn^{2+}. Note that it still contains Fe^{3+} and O^{2-}, therefore is an iron oxide-based NP. It had a mean individual core size of 15.4 nm, as determined by TEM; however, due to particle agglomeration and the citrate layer, the mean

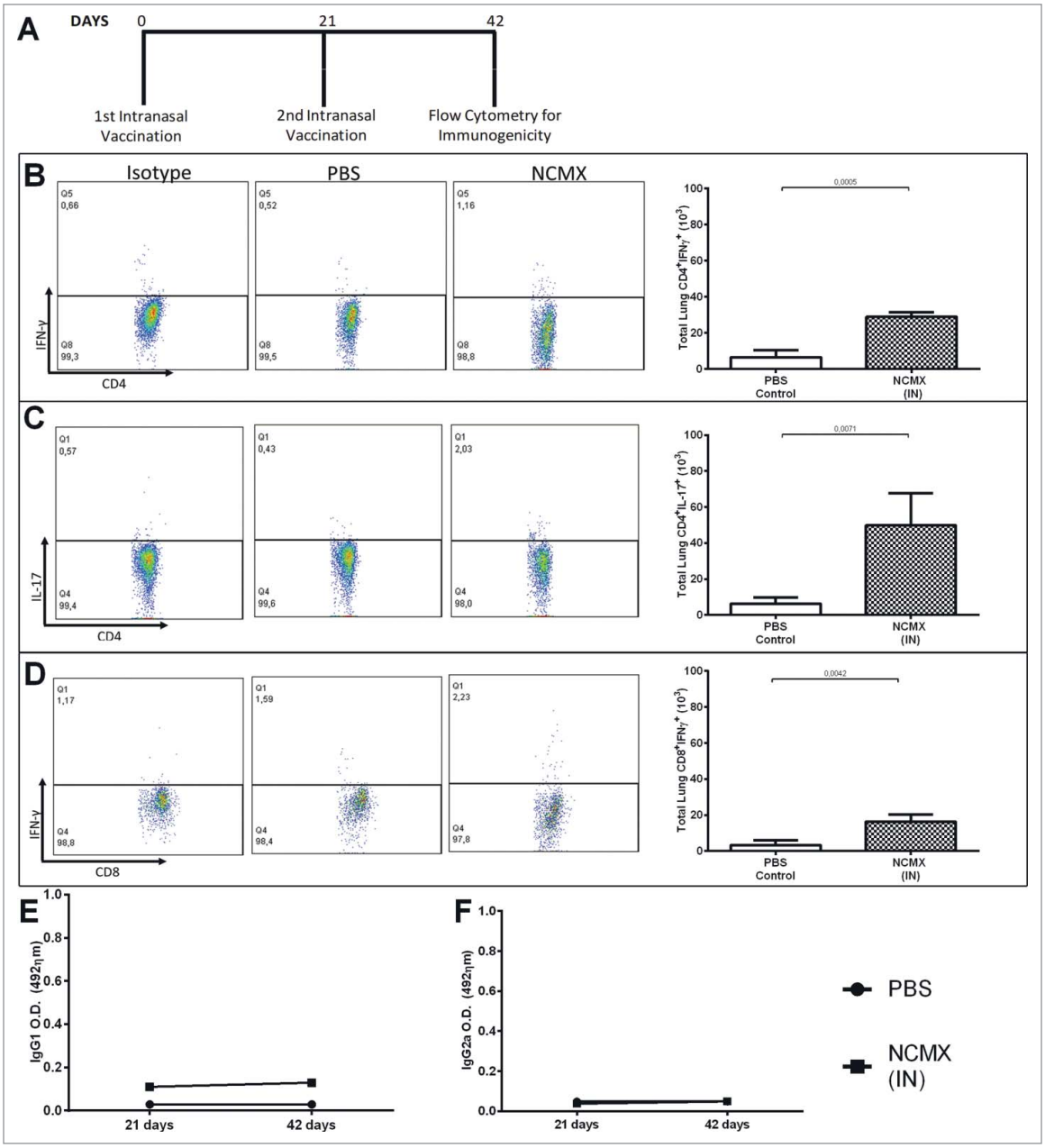

Figure 5. Intranasal vaccination increases the cellular immune response in the mucosa. (A) Mice were vaccinated 2 times at 21-day intervals with NCMX. At 21 days after the last immunization, the lungs were collected and analyzed by flow cytometry for (B) Th1 ($CD4^+IFN\text{-}\gamma^+$), (C) Th17 ($CD4^+IL\text{-}17^+$), and (D) Tc1 ($CD8^+IFN\text{-}\gamma^+$) cells. Mouse serum samples were collected 21 days after each vaccination for evaluation of the elicited humoral immune response by measuring the levels of IgG1 (E) and IgG2a (F). Differences between the means of the groups were determined by Student's *t*-test, and p values are shown. Significant differences were found between the groups, n = 4.

hydrodynamic diameter was larger, on the order of 85.9 nm in phosphate-buffered saline (PBS), which was the vaccine buffer. The immune responses elicited by metallic NPs have been shown to be related to the size and shape of the NPs, as demonstrated by Niikura (2013)[35]; however, in that study, only gold NPs and TNF-α and antibody responses were investigated, and these NPs may have significantly different properties than our NPs. Consequently, the effect of the physical characteristics of metallic NPs (such as IONPs or Mn-doped iron oxide NPs) on the immune response remains to be elucidated.

The formation of a protein corona composed of the fusion protein CMX was also demonstrated, along with NP agglomeration; the particle size increased to more than 600 nm (DLS) and 800 nm (FEG-SEM) after protein adsorption. The larger NPs can serve as a depot at the vaccine inoculation site, guiding the immune response to the site and prolonging antigen release, and consequently, antigen presentation, thereby having a direct impact on lymph node drainage, cellular uptake, and antigen presentation.[36] NPs larger than 500 nm have been shown to need DCs to reach lymph nodes from the injection site,[37] and NPs exhibiting the depot effect (in a cationic liposome model)

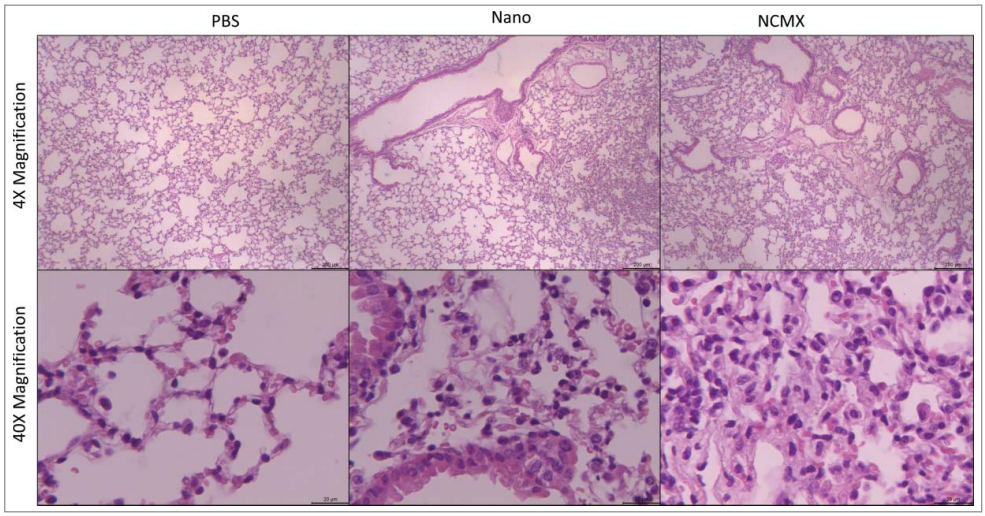

Figure 6. Evaluation of lung injury or tissue changes in intranasally vaccinated mice. Mice were vaccinated 2 times at 21-day intervals with NCMX. At 21 days after the last immunization, the lungs were collected, stained with H&E and analyzed for damage at 4x magnification (upper) and 40x magnification (botton).

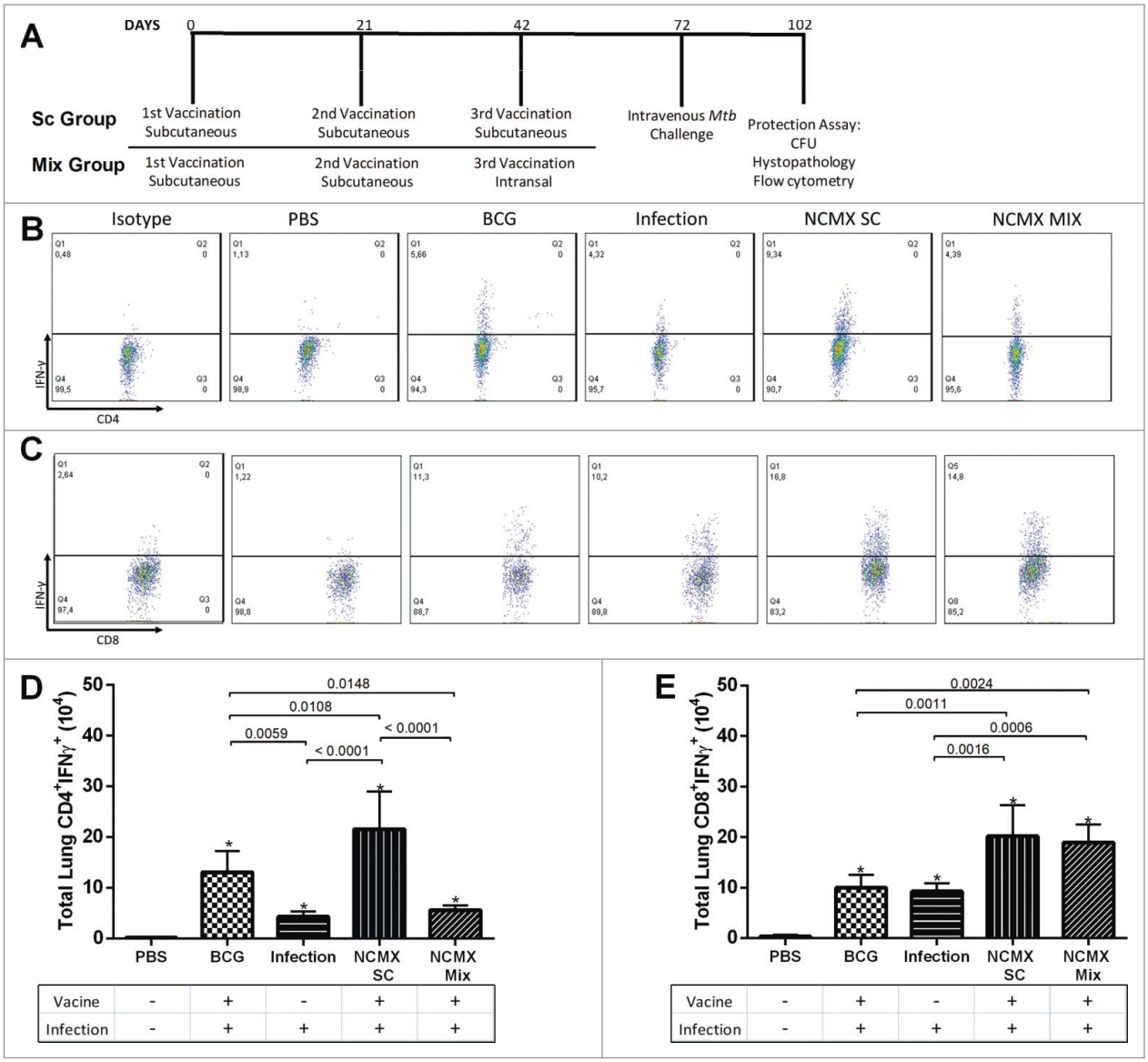

Figure 7. Challenge with Mtb after vaccination with NCMX recalls Th1 and Tc1 populations to the lungs. Thirty days after the challenge (A), the lungs were analyzed for the presence of $CD4^+IFN\text{-}\gamma^+$ (B) and $CD8^+IFN\text{-}\gamma^+$ (C) lymphocytes to evaluate the capacity of the immune cells generated by the vaccination to migrate to the lungs and to help protect against infection. The total number of cells was then calculated and is summarized in the graph below the dot plot for $CD4^+IFN\text{-}\gamma^+$ (D) and $CD8^+IFN\text{-}\gamma^+$ (E) cells. Differences among the groups were determined by one-way ANOVA, and p values are shown. Significant differences were found among the groups, $n = 4$.

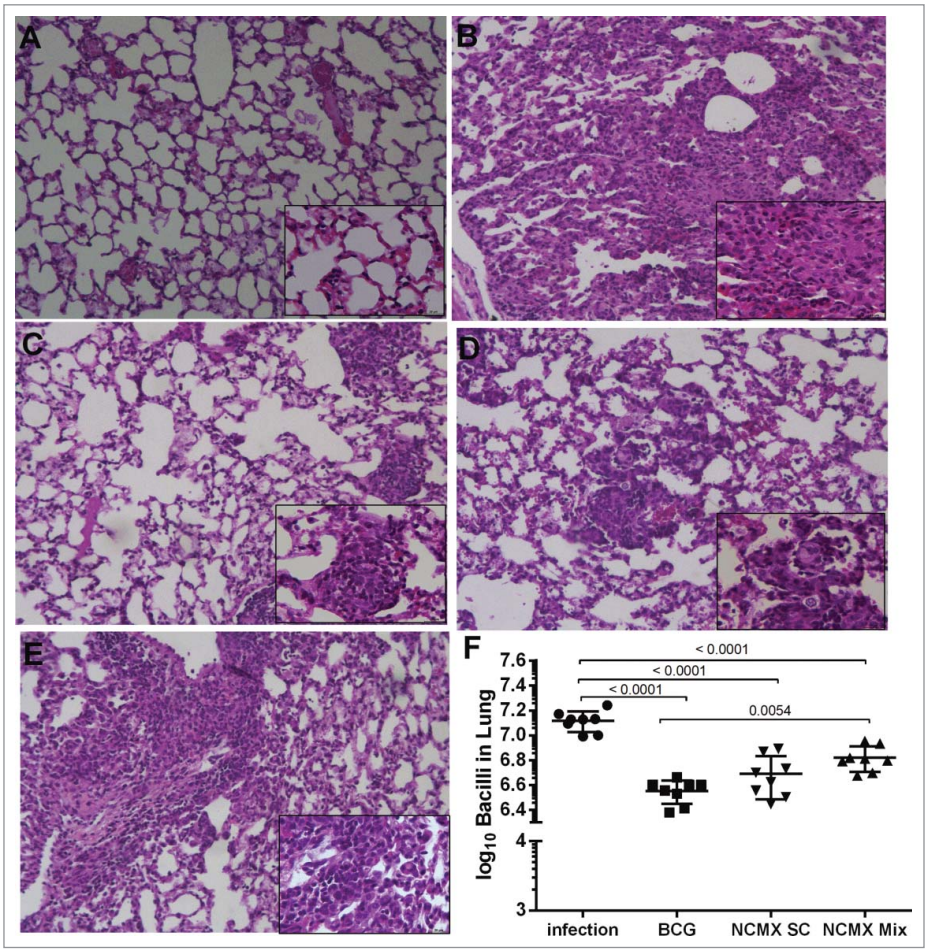

Figure 8. Vaccination with NCMX reduced the histopathological damage and bacterial load in the lungs of Mtb-challenged mice. Thirty days after the last vaccination via subcutaneous and mixed administration, mice were challenged with 10^6 CFU per animal. After thirty days, the mice were euthanized, and the lungs were studied to determine the capacity of the vaccination to protect against damage and pathological response (A to E), as well as its capacity to diminish the bacterial load in the lungs (F). Lung samples were also stained with H&E and analyzed for damage at 4x magnification and 40x magnification. Differences among the mean CFU values were determined by one-way ANOVA, and p values are shown. Significant differences were demonstrated among the groups, n = 8.

have been shown to be more capable of inducing IFN-γ release.[38]

We verified the possibility of using different doses of NPs in vaccine formulations (10 μg and 50 μg). Both doses generated Th1 and Tc1 responses; thus, the NP dose seems to have less of an impact on cellular immunity than on the humoral immune response (Fig. 2). Sindrilaru et al. (2011) have shown that greater iron uptake by macrophages makes the macrophages less modulatory and capable of secreting more proinflammatory cytokines.[38] Similar to iron, manganese has also been demonstrated to be capable of inducing proinflammatory responses in microglia; however, manganese alone induced moderate only production of IL-6 and TNF-α,[39] as well as superoxide reactivity, H_2O_2 formation and NO production by neutrophils.[40] Therefore, the use of higher concentrations of iron and manganese-based NPs could be directly correlated with the immune response induced. Yet, from our data, the tendency of the particles to induce a greater CD8 response when 50 μg was used indicates that the NP dose should be investigated to better understand this relationship.

The administration route can affect the immune response elicited by a vaccine. For instance, when mice are immunized through subcutaneous route, CD103+ DC subset present in the dermal compartment can migrate to the site of injection and then migrate to the LN. Dermal CD103+ DC produce IL-12 and can cross present the antigen by MHCII/MHCI generating Th1/Tc1 (CD8) responses.[41] Our results with subcutaneous vaccination also induced Th1/Tc1 responses and probably this was due to production of IL-12 by those DCs. Intranasal vaccination using NCMX generated Th1/Tc1 and Th17 responses, CD103+ DCs also present in the lungs could be involved in the generation of Th1/Tc1 responses.[42] Further, the DCs present in NALT (nasal associated lymphoid tissue) produce more IL-6 than those present in cervical lymph nodes and spleen and consequently might be responsible for preferential Th17 generation when the intranasal route was used.[32]

IONPs and $MnFe_2O_4$ NPs have been used in different nanomedical approaches and are usually tolerated well, sometimes at doses ten-fold higher than those used in this study.[10,43-45] However, repeated exposure of the airway to manganese (salt) or iron NPs can lead to pulmonary disorders, such as bronchiolitis and pneumonitis.[46-48] It is also through the airway that manganese enters the bloodstream and starts to accumulate in and damage the nervous system, leading to predispositions to neurodegenerative disorders.[47,49] Despite these disadvantages, passivation of the $MnFe_2O_4$ used here enriched the surface

with Fe, and the subsequent coating with CMX might have prevented the release of ions (Fe or Mn) during a short time window, thus reducing the toxicity. Not all adjuvants can be efficiently used for mucosal vaccine administration, and even established adjuvants, such as aluminum, MF-59 and even muramyl-di-peptide (cellular immune response adjuvant), have failed to induce an immune response via intranasal vaccination.[50] Thus, the diminished immunogenic capability of the intranasal route as a booster, with the need for multiple vaccinations through the same route, can be an obstacle for the use of NPs via this route, once mild inflammation of the lungs observed even after the second intranasal immunization.

To induce a CD8 response, the antigen should be presented by DCs to naïve CD8 cells via cross-presentation, and as demonstrated by Tran and Shen (2009),[51] NPs larger than 500 nm are better at inducing this type of response by reducing the endosomal pH and thus improving the antigen processing.[51] A TCD8 response can directly kill the infected cells or produce cytokines (Tc1) to aid in the activity of other cells[52]; the TCD8 response was the most prominent response induced by our vaccine formulation with NMCX. $CD8^+$ T cell generation is known to be partially CD4 independent; however, the development and maintenance of memory is CD4 dependent, and the priming of the Tc1 population is improved when correlated with the Th1 response.[53] In this study, even at low levels, the Th1 response was observed together with the Tc1 response.

The observed NCMX size of 622–881 nm implies that they will not be uptake by LECs. Therefore, the increase in the number of LECs observed in our experiments may be due to CMX antigen shedding and drainage to the lymph nodes that in turn could be taken by LECs. Previously, CMX alone was shown to induce activation of NF-κB, IL-6 and IL-1α.[25] Pusic and cols showed that iron oxide nanoparticles were capable of inducing IL-6, TNF-α, IL1-b, IFN-γ, and IL-12.[13] As shown by Tamburini and cols, although the adjuvant (polyIC) activates the innate immune response, only when the protein and the adjuvant formulation were used as vaccine LECs proliferated.[54] Thus maybe this is the case for our results, where the increase in the number of LECs was observed only when Nano was combined with CMX.

CMX is capable of inducing IL-6 and TGF-β expression in macrophages *in vitro*[25]; however, when used alone, it cannot generate an adaptive immune response.[55] This observation is in agreement with the literature showing that protein alone cannot efficiently generate an adaptive immune response.[56] CMX was used by de Sousa et al. (2010) in a formulation with CpG/DNA and liposomes and efficiently induced a Th1 response,[21] which is important for protection against TB. Compared with most potent adjuvants (such as lipopolysaccharide (LPS) or CpG/DNA), NPs have a diminished capacity for stimulating these types of responses,[13] but even without any TLR agonist, our formulation was able to induce a Th1 response.

The induction of the Th17 response is correlated with MHCII presentation and a milieu of IL-6 and TGF-β in the immunological synapse. This response is important for protection against TB by supporting Th1 reactivity and downregulating IL-10 and upregulating IL-12 production by DCs; after *Mtb* challenge, Th17 cells stimulate chemokine production, recruit $CD4^+$ T cells to the lungs, favor granuloma formation, and accelerate pathogen clearance.[30,57] CMX alone has been shown by da Costa et al. (2015) to induce IL-1α, IL-6 and TGF-β expression in bone marrow macrophages (BMMs), and iron NPs have also been demonstrated to be capable of inducing IL-6 and IL-β expression.[13,25] However, the stimulatory capacity of CMX is TLR-4 and TLR-2 dependent, and IONPs are capable of interfering with monocyte responses, diminishing the production of IL-1β and TNF-α, when used as co-stimuli with LPS (TLR-4 dependent).[58] This observation supports our finding of a low efficiency in the induction of a Th17 response by our formulations. Finally, we and others have recently demonstrated the role of IL-17 produced by Th17 cells in TB, and the failure to induce this population in this study was probable the main factor responsible for not achieving better protection against infection.

After the *Mtb* challenge, the subcutaneous and mixed formulations were able to recall the CD8 response, reflecting the capacity of the formulations to maintain and generate that response. Both recalled responses diminished the bacillary load in the lungs of infected mice, reinforcing the importance of this population in the protection against TB. However, the subcutaneous vaccination alone also induced a Th1 response that could be recalled upon challenge and diminished the damage to the lungs, demonstrating that the Th1/Tc1 immune response is responsible not only for killing the bacteria but also for delimiting and controlling the infection.[52,57]

The scientific community and the WHO have been careful with the use of metallic adjuvants, mainly because of the association of the presence of heavy metals in vaccines and adverse effects. However, there is no evidence of such adverse effects; for example, Taylor et al. (2014) evaluated almost 1.3 million people through a meta-analysis and found no evidence of an association between vaccination and autism.[59] In addition, the presence or absence of thimerosal (mercury-containing preservative) in American vaccines or immunoglobulin preparations does not affect the number of individuals with autism spectrum disorder.[60] Despite these observations, there are still questions about possible side effects. As such, we searched for potential toxic effects of our vaccine formulation; we found no hemolysis, and the vaccinated mice showed no evidence of organ damage or disease in terms of abnormal behavior, weight loss, reflexes, balance, exploration, strength, locomotor activity or any other parameter. The only observed effect was increased cellularity in the lungs when the mice were vaccinated intranasally, which is also correlated with cell migration and development of the immune response.

The biodistribution of nanoparticles can be related to several characteristics such as site of injection, size, shape and charge. Particularly, the size of the nanoparticle also dictates its distribution, once nanoparticle with size closest to the used in our work (600-800 nm) will be found almost equally in the lungs, liver and spleens, while nanoparticles smaller than 10 nm tend to be cleared by the kidneys.[61] Because of that, in toxicity assay we looked for any damage in the lungs, liver and kidneys of vaccinated mice. However, no sign of damage was found in any organ when NPs were utilized through subcutaneous route while only small modification was found in the lungs of animals vaccinated intranasally. Together with this, there are multiples possible cells which are capable of

endocytosis, as well as biodegrade these particles, particularly macrophages, dendritic cells and inflammatory monocytes.[62] The amount of NP in our formulations (50μg being the biggest quantity) is well below the amounts used in FDA approved iron oxide based formulations such as Feraheme or Resovist that can be used in mice from 0.6 mg to 12.3 mg, respectively.[63] Furthermore, even with this type of NP taking several weeks to be degraded, the administered amount are not capable to become toxic, while reports in the literature indicate that it can be used by the body as nutrient iron or be excreted in the feces after degradation.[64,65]

The formulation used here efficiently induced a Tc1 response, which heightens the potential use of this formulation (Tc1 inducer) in cases where the TCD4 response is not efficient, such as in AIDS. In addition, we only used NPs as an adjuvant and immunostimulant, and other approaches, for example, complexing with CpG/DNA or other TLR agonists, can improve the desired immune response. However, the use of such approaches must be carefully evaluated since the presence of NPs can alter the function and response of TLRs, as demonstrated for TLR-2 and TLR-4.[58]

In this study, we found distinct responses when different doses and routes were used, with SC50 generating more IgG1 and IgG2a than SC10. Vaccination strategies that included intranasal vaccination (alone or combined with subcutaneous) did not induce or improve significant antibody titers. In TB, the mechanism of antibody protection is unclear, but it seems to be essential for containing the mycobacterial infection by synergizing with cellular immune response.[66-68] In some studies, comparison of similarly shaped particles revealed an inverse correlation between the particle size and immune response, with smaller particles inducing a more efficient humoral response, while these effects were not observed in other studies.[34,69,70]

Although our cell preparations could contain circulating blood cells not representative of the investigated organ, the mucosal immune response was evaluated after perfusing the lungs with ice-cold PBS containing heparin to remove traces of blood.[71] Our group evaluated protection against TB using the intravenous route with relatively high bacillary doses, which is not the usual route of infection for TB but provides a better surrogate of protection due to the higher bacterial load rapidly achieved in several tissues following infection requiring a more efficient protective response that could be missed when low-dose aerosol infection is used.[22,72] BCG is always used as a control in our studies, and as shown by our results, the protection induced by BCG in our model of infection is similar to that obtained by several groups that work with vaccines and use the aerosol route of TB infection. Moreover, the lesions caused by intravenous infection are similar to those caused by aerosol infection; thus, the host-pathogen interactions are conserved.[23,24,55]

Finally, for the first time, this study demonstrates that $MnFe_2O_4$ NPs in a vaccine formulation can generate cellular immune responses. The formulation could generate Th1 and, most prominently, Tc1 (CD8) responses that could be recalled upon TB infection and could help in protection against the bacteria, as demonstrated by our evaluation of the total immune response present in the lungs and spleen.

Materials and methods

Ethics statement

This study was carried out in strict accordance with the recommendations of the Guide for the Care and Use of Laboratory Animals of the Committee of Sociedade Brasileira de Animais de Laboratório (SBAL). The animals were housed and handled according to the guidelines of the Conselho Nacional de Controle e Experimentação Animal (CONCEA). The protocol for this work was approved by the Committee on the Ethics of Animal Experiments of the University Federal de Goiás (protocol number: 103/14).

Citrate-coated $MnFe_2O_4$ NP synthesis and CMX coating

The citrated-coated $MnFe_2O_4$ NPs were synthesized as described by Nunes et al. (2014).[44] Briefly, 50 mmol of $FeCl_3$ and 25 mmol of $MnCl_2$ (both dissolved in 100 mL of 3% HCl) were introduced into 500 mL of boiling 2.0 mol/L methylamine solution under vigorous stirring for 30 min. The obtained solid was magnetically separated from the supernatant and washed three times with distilled water. The precipitate was acidified with a 0.5 mol/L HNO_3 solution and magnetically separated from the supernatant, which was discarded. Then, the NPs were hydrothermally treated by boiling 0.5 mol/L $Fe(NO_3)_3$ for 30 min, and the excess ferric nitrate was removed from the solution by magnetic decantation. After preparation of the magnetic composite, the coating process was performed by the addition of sodium citrate to the solution under stirring for 30 min using a 1:10 mass ratio of $Na_3C_6H_5O_7$ to $MnFe_2O_4$, in 50 mL of water. The obtained precipitates were magnetically separated, and the supernatants were discarded. Then, the precipitates were washed three times with acetone, the desired amount of water was added, and the excess acetone was evaporated to yield the magnetic fluid samples.

CMX protein is a recombinant protein developed by de Sousa et al. (2012)[21] and produced in Escherichia coli in the Immunopathology and Infectious Diseases Laboratory at the Institute of Tropical Pathology and Public Health (Instituto de Patologia Tropical e Saúde Pública – IPTSP), UFG.

For the CMX coating, we utilized the protocol of Yang and Burkhard (2012)[73] with modifications. Briefly, $MnFe_2O_4$ NPs were diluted in the CMX protein solution (200 μg/mL antigen concentration) to a concentration of 100 μg/ml (SC 10) or 500 μg/mL (SC 50). The solution was then incubated for 2 h under 1000 rpm homogenization and utilized for the other tests and in immunizations.

Characterization of NPs with and without CMX protein corona

The hydrodynamic diameter of citrate-coated $MnFe_2O_4$ NPs and citrate-coated $MnFe_2O_4$ NPs coated with CMX (NCMX) was determined with a Malvern Zetasizer Nano S equipped with a 633-nm laser (Instituto de Química – Laboratório de Química Analítica -UFG). Hellma quartz cuvettes with a 3-mm path length and a 9.65-mm center were used. Measurements were performed at 20°C using 500-μL samples. The hydrodynamic diameters were verified by Malvern DTS software, version 7.01.

In addition, the size of the citrate-coated $MnFe_2O_4$ NPs was characterized by TEM. A drop of the NP solution was deposited onto a glow-discharged carbon-coated grid. The grid was subsequently dried and visualized using a JEOL JSM-6610 microscope (JEOL, Japan) equipped with an energy dispersive spectrometer (EDS; Thermo Fisher Scientific NSS Spectral Imaging) at Laboratório de Microscopia de Alta Resolução LabMic – UFG). The images were analyzed with public domain Java ImageJ software (V1.37).[74] For the NP size measurements by TEM, 230 NPs were evaluated.

The process of coating the NP surface with protein is known in the literature as protein corona formation.[75] To visualize the CMX corona formation, the NCMX suspension was dripped onto ultra-thin carbon membranes and left to dry at room temperature to make the membranes suitable for analysis. The images were acquired using a JEOL JSM-7100F field-emission scanning electron microscope in scanning transmission electron microscope (FE-SEM) mode at Centro Regional de Desenvolvimento Tecnológico (CRTI-UFG). For each sample, a series of images with increasing magnification was recorded. The images were analyzed, and the corona was evaluated using public domain Java ImageJ software (V1.37).[74]

NCMX samples were separated by lateral magnetic separation for 24 h and resuspended in PBS (100 μL). To evaluate unbound protein, the residual supernatant from the lateral magnetic separation was centrifuged at 16,000 × g for 15 min at 22°C. Then, the supernatant was discarded, and the sediment was resuspended in PBS and applied to a nitrocellulose membrane.

For the immunodot blot assay, a nitrocellulose membrane was spotted with 10 μL of each of the following solutions: a solution containing 5 μg of NPs, a solution containing 10 μg of CMX, 10 μL of the NCMX formulation and 10 μL of the lateral flow NP separation supernatant. After this step, the nitrocellulose membrane was incubated with polyclonal antiserum against CMX (1:10,000 dilution obtained from rCMX-immunized BALB/c mice). The membrane was then incubated with horseradish-peroxidase-conjugated anti-mouse IgG (Sigma-Aldrich). The presence of the CMX protein was detected by incubation with diaminobenzidine (Roche).

Protein corona quantification

Western blotting (Fig. 1C) was performed to quantify the recombinant CMX protein linked to the $MnFe_2O_4$ NPs. To release the protein corona from the NPs, NPs in NCMX (500 μL) were separated by lateral magnetic separation for 24 h. Then, the supernatant was discarded, and the sediment was resuspended in 500 μL of 10% SDS-PBS buffer, incubated for 30 min, and centrifuged at 5000 rpm for 10 min; then, 10 μL of the supernatant was utilized for western blotting. After transferring the proteins to the nitrocellulose membrane, the procedures described above were followed to perform the immunodot blot assay.

Animals

Specific-pathogen-free female BALB/c mice (4–8 weeks old), purchased from CEMIB-UNICAMP, were maintained in ABSL-2 racks fitted with a HEPA-filtered air intake and exhaust system with water and food provided ad libitum at the animal care facility of the Institute of Tropical Pathology and Public Health at Federal University of Goiás. The temperature was maintained from 20–24°C with a relative humidity of 40–70% and a 12-h light/dark cycle. This study was carried out in strict accordance with the recommendations of the Guide for the Care and Use of Laboratory Animals of the Committee of SBAL and was approved by the Research Ethical Committee of Federal University of Goiás (approval number: 103/14).

Immunogenicity assay

Three vaccination strategies, with 21-day intervals between immunizations, were performed. The first strategy, to define the vaccine dose, consisted of mice immunized SC three times. Two vaccine formulations were utilized, as follows: (I) the SC10 group utilized 10 μg of NPs mixed with 20 μg of CMX per animal; (II) the SC50 group utilized 50 μg of NPs mixed with 20 μg of CMX per animal. The second strategy consisted of two subcutaneous immunizations with 100 μL of the NCMX formulation (10 μg of NPs mixed with 20 μg of CMX) per animal followed by an additional booster via intranasal instillation at the same dose as the subcutaneous injection. The third vaccination scheme was performed using two intranasal instillations of 100 μL of the NCMX formulation (10 μg of NPs mixed with 20 μg of CMX) per animal.

Twenty-one days after the last immunization, the mice were euthanized, and the lungs and spleens were collected for flow cytometry analysis and histological immune response evaluation. As a negative control, a group of mice received PBS (100 μL) via the same routes evaluated in each experimental strategy.

Serum collection and ELISA

Serum samples were collected from the immunized mice 21 days after each immunization. The samples were incubated for 1 h at 37°C, centrifuged at 1,200 × g for 15 min at 4°C to separate the serum, and stored at -20°C.

ELISA was performed as described by Sousa et al. (2012).[21] Briefly, 96-well polystyrene plates (Falcon®) were coated with 10 μg/mL of recombinant CMX fusion protein diluted in 0.05 M sodium carbonate/bicarbonate buffer and incubated at 4°C for 16 h. The wells were blocked with PBS containing 1% skim milk. The serum samples were diluted 1:40, added to the wells, and incubated for 2 h at 37°C. Biotin-conjugated antibodies (anti-IgG1 or anti-mouse IgG2a; Pharmingen®) diluted 1:5000 were added to the plates, which were then incubated for 1 h at 37°C. Streptavidin peroxidase, diluted 1:1000, was added, and the plates were incubated again for 1 h at 37°C. After incubation with the substrate solution, the absorbance at 492 nm was measured on an ELISA reader (LabSystems Multiskan Thermo®).

CMX-specific cellular responses in the lungs and spleen

Cell preparation and the cytometry protocol were performed as described by Junqueira-Kipnis et al. (2013) and

da Costa et al. (2014).[22,23] Briefly, twenty-one days after the last immunization, four BALB/c mice from each group were euthanized, and the spleens and lung lobes were collected. The spleens were prepared as single-cell suspensions using 70-μm cell strainers (BD Biosciences), and the cells were resuspended in RPMI medium. After erythrocytes were lysed with lysis solution (0.15 M NH_4Cl, 10 mM $KHCO_3$), the cells were washed and resuspended in RPMI medium supplemented with 10% fetal calf serum, 0.15% sodium bicarbonate, 1% L-glutamine (200 mM; Sigma-Aldrich), and 1% nonessential amino acids (Sigma-Aldrich). Cells were counted in a Neubauer chamber, and the concentration was adjusted to 1×10^6 cells/mL. Prior to collection, the lungs were perfused with ice-cold PBS containing 45 U/mL heparin (Sigma-Aldrich). The lungs were digested with DNAse IV (30 μg/mL; Sigma-Aldrich) and collagenase III (0.7 mg/mL; Sigma-Aldrich Brazil) for 30 min at 37°C. The digested lungs were prepared as single-cell suspensions using 70-μm cell strainers and subjected to erythrocyte lysis. The cells were washed and resuspended in RPMI medium, and the concentration was adjusted to 1×10^6 cells/mL.

Cell stimulation was performed in a 96-well cell-culture plate (CellWells™). Spleen or lung cell suspensions were cultivated with media alone, with recombinant CMX (10 μg) or with ConA (positive control) in a 5% CO_2 incubator at 37°C for 4 h. Then, monensin (3 μM; eBioscience) was added to the wells, and the cultures were incubated for 4 h. Cells were treated with 0.1% sodium azide in PBS for 30 min at room temperature and then centrifuged. The cells were stained with FITC-conjugated anti-CD4 (BD Pharmingen; clone RM4-5) or PE-conjugated anti-CD8 for 30 min and then permeabilized with Perm Fix/Perm Wash (BD Pharmingen), washed with 0.1% sodium azide in PBS, and stained with the following antibodies for 30 min to assess the expression of a panel of Th1/Th17 cytokines: PerCP-conjugated anti-IL-17A (eBioscience; clone: eBio17B7) and APC-conjugated anti-IFN-γ (eBioscience; clone: XMG1.2). Cell acquisition at 50,000 events per sample was performed using a BD FACS Verse (Universidade Federal de Goiás, Instituto de Patologia Tropical e Saúde Pública) flow cytometer, and the acquired data were analyzed using FlowJo (V10) software.

LEC evaluation

Specific-pathogen-free female BALB/c mice (4–8 weeks old) were injected SC in the dorsal region with PBS (saline; 100 μL), CMX (20 μg), $MnFe_2O_4$ NPs (10 μg), or NCMX (SC10) prepared as described above. At 1 or 4 days after inoculation, the mice were euthanized, and the axillary lymph nodes were collected and prepared as single-cell suspensions using 70-μm cell strainers (BD Biosciences); the cells were resuspended with RPMI medium supplemented with 20% fetal calf serum, 0.15% sodium bicarbonate, 1% L-glutamine (200 mM; Sigma-Aldrich), and 1% nonessential amino acids (Sigma-Aldrich). The cells were counted in a Neubauer chamber, and the concentration was adjusted to 1×10^6 cells/mL. For staining, the cells were centrifuged and then stained with FITC-conjugated anti-gp38 (clone: 8.1.1; Novus Biologicals) and PE-Cy7-conjugated anti-CD31 (BD bioscience; clone: 390) for 30 min. Cell acquisition at 100,000 events per sample was performed using a BD FACS Verse system, as previously described. LECs were characterized as $gp38^+CD31^+$, as described by Tamburini et al. (2014).[54]

Intravenous infection with Mtb

The Mtb H37Rv strain was maintained as previously described (Junqueira-Kipnis et al., 2013).[22] A vial from a constant stock was thawed, and the inoculum was adjusted to a concentration of 10^6 CFU/mL by dilution with PBS containing 0.05% Tween 80. The immunized animals were challenged with 10^5 bacilli. Thirty days after immunization, 100 μL of the inoculum was injected into the tail vein. The inoculum/infective bacterial load was determined by plating the lung homogenates on 7H11 agar supplemented with OADC for one mouse in each group on day one after infection. Thirty days after infection, the mice were euthanized, and the anterior and mediastinal right-lung lobes were collected, homogenized, and plated on 7H11 agar supplemented with OADC. The bacterial load was determined by counting the CFU after 21 days of incubation at 37°C.

Histopathology

To assess the possibility of vaccination inducing organ inflammation or causing side effects, mice were euthanized 21 days after the 2 intranasal vaccinations and after 2 and three subcutaneous vaccinations, and the lungs (Fig. 4), heart, kidneys and liver (Supplementary Fig. 3) were collected for histology. To evaluate the ability of the generated immune response to protect against the pathogenic effect of infection, mice were euthanized 30 days after being challenged with *Mtb*. For histological evaluation of the lungs, the organs were perfused with 0.05% heparin by injection in the right ventricle of the heart, and the caudal right lobes were collected. The lungs, heart, kidneys and liver were conditioned in histological cassettes and fixed with 10% buffered formaldehyde. Samples were sectioned at a thickness of 5 μm and stained with H&E for analysis by optical microscopy (Axio Scope.A1, Zeiss). Two representative images (4x,10x or 40x) for each group were acquired.

Hemolysis assay

Blood from a healthy patient was collected (5 mL) in a heparinized tube, and red blood cells were separated and washed with PBS. The red blood cell volume was adjusted to 2% at a concentration of 1×10^8 cells/mL. Concentrations of 10, 50, 100 and 500 μg of $MnFe_2O_4$ NPs, i.e., concentrations up to 50-fold greater than the value used in the vaccine (10 or 50 μg), were prepared for volume/volume addition (100 mL) with the red blood cells. Cells were incubated for 1 h at 37°C and centrifuged (1000 g); then, the absorbance at 550 nm was determined. As a positive control, the erythrocytes were treated with Triton-100X, and as a negative control, PBS was added. The percentage of red blood cell hemolysis was obtained by the following formula: % hemolysis = 100X [(Sample – AbsPBS) / (AbsTriton – AbsPBS)].

Statistical analysis

The results were tabulated using Excel and Prism software (version 7.0, GraphPad). The differences between groups were assessed with a nonparametric Student's *t*-test or one-way ANOVA followed by Dunn's post hoc test. Significant differences were found among the groups. All three repetitions of the experiments showed similar responses. The size distribution of the NPs was evaluated by the Anderson-Darling normality test.

Disclosure of potential conflicts of interest

The authors declare that the research was conducted in the absence of any commercial or financial relationships that could be construed as a potential conflict of interest.

Acknowledgments

This work is part of the PhD thesis of Lázaro Moreira Marques Neto in the Biotechnology and Biodiversity Graduate Program at CAPES. The authors would like to thank the Labmic Core Facility from the Universidade Federal de Goiás for use of the scanning electron microscope.

Funding

This work was funded by FAPEG (grant number: 2013.10267001143), CNPq (grant number: 405198/2015-9) and CAPES (grant number: 88887.108519/2015-01) . LMMN received a PhD fellowship from CAPES (88882.161533/2017-01), and APJK (#303675/2015-2) and AK (#307186/2013-0) received a productivity research fellowship from CNPq.

Author contributions

LMM performed all the experiments and wrote the draft. APJK conceived the experiments. NZ, AAS and AFB developed and characterized the NPs. MMT and ACC developed the toxicity experiments. AFB, AK and APJK critically revised the manuscript. All authors have read the final version of the manuscript.

ORCID

Lázaro Moreira Marques Neto http://orcid.org/0000-0003-0760-0044
Ailton Antônio de Sousa-Júnior http://orcid.org/0000-0001-8216-2043
André Kipnis http://orcid.org/0000-0001-5950-106X

References

1. Shah RR, Hassett KJ, Brito LA. Overview of Vaccine Adjuvants: Introduction, History, and Current Status. Methods Mol Biol. 2017;1494:1–13. doi:10.1007/978-1-4939-6445-1_1.
2. Andersen P, Urdahl KB. TB vaccines; promoting rapid and durable protection in the lung. Curr Opin Immunol. 2015;35:55–62. doi:10.1016/j.coi.2015.06.001.
3. Wang X, Zhang J, Liang J, Zhang Y, Teng X, Yuan X, Fan X. Protection against Mycobacterium tuberculosis infection offered by a new multistage subunit vaccine correlates with increased number of IFN-gamma+ IL-2+ CD4+ and IFN-gamma+ CD8+ T cells. PLoS One. 2015;10:e0122560. doi:10.1371/journal.pone.0122560.
4. Xu Y, Yang E, Huang Q, Ni W, Kong C, Liu G, Li G, Su H, Wang H. PPE57 induces activation of macrophages and drives Th1-type immune responses through TLR2. J Mol Med (Berl). 2015;93:645–62. doi:10.1007/s00109-014-1243-1.
5. Belyakov IM, Ahlers JD. What role does the route of immunization play in the generation of protective immunity against mucosal pathogens? J Immunol. 2009;183:6883–92. doi:10.4049/jimmunol.0901466.
6. Salem AK. Nanoparticles in vaccine delivery. AAPS J. 2015;17:289–91. doi:10.1208/s12248-015-9720-1.
7. Branquinho LC, Carriao MS, Costa AS, Zufelato N, Sousa MH, Miotto R, Ivkov R, Bakuzis AF. Effect of magnetic dipolar interactions on nanoparticle heating efficiency: implications for cancer hyperthermia. Sci Rep. 2013;3:2887. doi:10.1038/srep02887.
8. Ludwig F, Eberbeck D, Lowa N, Steinhoff U, Wawrzik T, Schilling M, Trahms L. Characterization of magnetic nanoparticle systems with respect to their magnetic particle imaging performance. Biomed Tech (Berl). 2013;58:535–45. doi:10.1515/bmt-2013-0013.
9. Hola K, Markova Z, Zoppellaro G, Tucek J, Zboril R. Tailored functionalization of iron oxide nanoparticles for MRI, drug delivery, magnetic separation and immobilization of biosubstances. Biotechnol Adv. 2015;33:1162–76. doi:10.1016/j.biotechadv.2015.02.003.
10. Quini CC, Prospero AG, Calabresi MFF, Moretto GM, Zufelato N, Krishnan S, Pina DR, Oliveira RB, Baffa O, Bakuzis AF, et al. Real-time liver uptake and biodistribution of magnetic nanoparticles determined by AC biosusceptometry. Nanomedicine. 2017;13:1519–29. doi:10.1016/j.nano.2017.02.005.
11. Fang RH, Zhang L. Nanoparticle-Based Modulation of the Immune System. Annu Rev Chem Biomol Eng. 2016;7:305–26. doi:10.1146/annurev-chembioeng-080615-034446.
12. Marques Neto LM, Kipnis A, Junqueira-Kipnis AP. Role of metallic nanoparticles in vaccinology: Implications for infectious disease vaccine development. Front Immunol. 2017;8:239. doi:10.3389/fimmu.2017.00239.
13. Pusic K, Aguilar Z, McLoughlin J, Kobuch S, Xu H, Tsang M, Wang A, Hui G. Iron oxide nanoparticles as a clinically acceptable delivery platform for a recombinant blood-stage human malaria vaccine. FASEB J. 2013;27:1153–66. doi:10.1096/fj.12-218362.
14. Zumla A, George A, Sharma V, Herbert RH, Baroness Masham of I, Oxley A, Oliver M. The WHO 2014 global tuberculosis report–further to go. Lancet Glob Health. 2015;3:e10–2. doi:10.1016/S2214-109X(14)70361-4.
15. Kaufmann SH, Weiner J, von Reyn CF. Novel approaches to tuberculosis vaccine development. Int J Infect Dis. 2017;56:263–7. doi:10.1016/j.ijid.2016.10.018.
16. Warrier T, Tropis M, Werngren J, Diehl A, Gengenbacher M, Schlegel B, Schade M, Oschkinat H, Daffe M, Hoffner S, et al. Antigen 85C inhibition restricts Mycobacterium tuberculosis growth through disruption of cord factor biosynthesis. Antimicrob Agents Chemother. 2012;56:1735–43. doi:10.1128/AAC.05742-11.
17. Rinke de Wit TF, Bekelie S, Osland A, Wieles B, Janson AA, Thole JE. The Mycobacterium leprae antigen 85 complex gene family: identification of the genes for the 85A, 85C, and related MPT51 proteins. Infect Immun. 1993;61:3642–7.
18. Ramalingam B, Baulard AR, Locht C, Narayanan PR, Raja A. Cloning, expression, and purification of the 27 kDa (MPT51, Rv3803c) protein of Mycobacterium tuberculosis. Protein Expr Purif. 2004;36:53–60. doi:10.1016/j.pep.2004.01.016.
19. Haile Y, Bjune G, Wiker HG. Expression of the mceA, esat-6 and hspX genes in Mycobacterium tuberculosis and their responses to aerobic conditions and to restricted oxygen supply. Microbiology. 2002;148:3881–6. doi:10.1099/00221287-148-12-3881.
20. Hu Y, Movahedzadeh F, Stoker NG, Coates AR. Deletion of the Mycobacterium tuberculosis alpha-crystallin-like hspX gene causes increased bacterial growth in vivo. Infect Immun. 2006;74:861–8. doi:10.1128/IAI.74.2.861-868.2006.
21. de Sousa EM, da Costa AC, Trentini MM, de Araujo Filho JA, Kipnis A, Junqueira-Kipnis AP. Immunogenicity of a fusion protein containing immunodominant epitopes of Ag85C, MPT51, and HspX from Mycobacterium tuberculosis in mice and active TB infection. PLoS One. 2012;7:e47781. doi:10.1371/journal.pone.0047781.
22. Junqueira-Kipnis AP, de Oliveira FM, Trentini MM, Tiwari S, Chen B, Resende DP, Silva BD, Chen M, Tesfa L, Jacobs WR, Jr, et al. Prime-boost with Mycobacterium smegmatis recombinant vaccine improves protection in mice infected with Mycobacterium tuberculosis. PLoS One. 2013;8:e78639. doi:10.1371/journal.pone.0078639.
23. da Costa AC, Costa-Junior Ade O, de Oliveira FM, Nogueira SV, Rosa JD, Resende DP, Kipnis A, Junqueira-Kipnis AP. A new recombinant BCG vaccine induces specific Th17 and Th1 effector cells with higher

protective efficacy against tuberculosis. PLoS One. 2014;9:e112848. doi:10.1371/journal.pone.0112848.
24. Oliveira FM, Trentini MM, Junqueira-Kipnis AP, Kipnis A. The mc2-CMX vaccine induces an enhanced immune response against Mycobacterium tuberculosis compared to Bacillus Calmette-Guerin but with similar lung inflammatory effects. Mem Inst Oswaldo Cruz. 2016;111:223–31. doi:10.1590/0074-02760150411.
25. da Costa AC, de Resende DP, Santos BPO, Zoccal KF, Faccioli LH, Kipnis A, Junqueira-Kipnis AP. Modulation of Macrophage Responses by CMX, a Fusion Protein Composed of Ag85c, MPT51, and HspX from Mycobacterium tuberculosis. Front Microbiol. 2017;8:623.
26. Mikhak Z, Strassner JP, Luster AD. Lung dendritic cells imprint T cell lung homing and promote lung immunity through the chemokine receptor CCR4. J Exp Med. 2013;210:1855–69. doi:10.1084/jem.20130091.
27. Chen L, Wang J, Zganiacz A, Xing Z. Single intranasal mucosal Mycobacterium bovis BCG vaccination confers improved protection compared to subcutaneous vaccination against pulmonary tuberculosis. Infect Immun. 2004;72:238–46. doi:10.1128/IAI.72.1.238-246.2004.
28. Darrah PA, Bolton DL, Lackner AA, Kaushal D, Aye PP, Mehra S, Blanchard JL, Didier PJ, Roy CJ, Rao SS, et al. Aerosol vaccination with AERAS-402 elicits robust cellular immune responses in the lungs of rhesus macaques but fails to protect against high-dose Mycobacterium tuberculosis challenge. J Immunol. 2014;193:1799–811. doi:10.4049/jimmunol.1400676.
29. Orr MT, Beebe EA, Hudson TE, Argilla D, Huang PW, Reese VA, Fox CB, Reed SG, Coler RN. Mucosal delivery switches the response to an adjuvanted tuberculosis vaccine from systemic TH1 to tissue-resident TH17 responses without impacting the protective efficacy. Vaccine. 2015;33:6570–8. doi:10.1016/j.vaccine.2015.10.115.
30. Trentini MM, de Oliveira FM, Kipnis A, Junqueira-Kipnis AP. The role of neutrophils in the induction of specific Th1 and Th17 during vaccination against tuberculosis. Front Microbiol. 2016;7:898. doi:10.3389/fmicb.2016.00898.
31. Monin L, Griffiths KL, Slight S, Lin Y, Rangel-Moreno J, Khader SA. Immune requirements for protective Th17 recall responses to Mycobacterium tuberculosis challenge. Mucosal Immunol. 2015;8:1099–109. doi:10.1038/mi.2014.136.
32. Zygmunt BM, Rharbaoui F, Groebe L, Guzman CA. Intranasal immunization promotes th17 immune responses. J Immunol. 2009;183:6933–8. doi:10.4049/jimmunol.0901144.
33. Wern JE, Sorensen MR, Olsen AW, Andersen P, Follmann F. Simultaneous Subcutaneous and Intranasal Administration of a CAF01-Adjuvanted Chlamydia Vaccine Elicits Elevated IgA and Protective Th1/Th17 Responses in the Genital Tract. Front Immunol. 2017;8:569. doi:10.3389/fimmu.2017.00569.
34. Rodriguez-Del Rio E, Marradi M, Calderon-Gonzalez R, Frande-Cabanes E, Penades S, Petrovsky N, Alvarez-Dominguez C. A gold glyco-nanoparticle carrying a Listeriolysin O peptide and formulated with Advax delta inulin adjuvant induces robust T-cell protection against listeria infection. Vaccine. 2015;33:1465–73. doi:10.1016/j.vaccine.2015.01.062.
35. Niikura K, Matsunaga T, Suzuki T, Kobayashi S, Yamaguchi H, Orba Y, Kawaguchi A, Hasegawa H, Kajino K, Ninomiya T, et al. Gold nanoparticles as a vaccine platform: influence of size and shape on immunological responses in vitro and in vivo. ACS Nano. 2013;7:3926–38. doi:10.1021/nn3057005.
36. Oyewumi MO, Kumar A, Cui ZR. Nano-microparticles as immune adjuvants: correlating particle sizes and the resultant immune responses. Exp Rev Vaccines. 2010;9:1095–107. doi:10.1586/erv.10.89.
37. Manolova V, Flace A, Bauer M, Schwarz K, Saudan P, Bachmann MF. Nanoparticles target distinct dendritic cell populations according to their size. European J Immunol. 2008;38:1404–13. doi:10.1002/eji.200737984.
38. Henriksen-Lacey M, Christensen D, Bramwell VW, Lindenstrom T, Agger EM, Andersen P, et al. Comparison of the Depot Effect and Immunogenicity of Liposomes Based on Dimethyldioctadecylammonium (DDA), 3 beta[N ‘,N ’-Dimethylaminoethane)carbomyl] Cholesterol (DC-Chol), and 1,2-Dioleoyl-3-trimethylammonium Propane (DOTAP): Prolonged Liposome Retention Mediates Stronger Th1 responses. Mol Pharmaceutics. 2011;8:153–61. doi:10.1021/mp100208f.
39. Sindrilaru A, Peters T, Wieschalka S, Baican C, Baican A, Peter H, Hainzl A, Schatz S, Qi Y, Schlecht A, et al. An unrestrained proinflammatory M1 macrophage population induced by iron impairs wound healing in humans and mice. J Clin Invest. 2011;121:985–97. doi:10.1172/JCI44490.
40. Filipov NM, Seegal RF, Lawrence DA. Manganese potentiates in vitro production of proinflammatory cytokines and nitric oxide by microglia through a nuclear factor kappa B-dependent mechanism. Toxicological Sci. 2005;84:139–48. doi:10.1093/toxsci/kfi055.
41. Apte SH, Redmond AM, Groves PL, Schussek S, Pattinson DJ, Doolan DL. Subcutaneous cholera toxin exposure induces potent CD103(+) dermal dendritic cell activation and migration. Eur J Immunol. 2013;43:2707–17. doi:10.1002/eji.201343475.
42. del Rio ML, Bernhardt G, Rodriguez-Barbosa JI, Forster R. Development and functional specialization of CD103+ dendritic cells. Immunol Rev. 2010;234:268–81. doi:10.1111/j.0105-2896.2009.00874.x.
43. Felton C, Karmakar A, Gartia Y, Ramidi P, Biris AS, Ghosh A. Magnetic nanoparticles as contrast agents in biomedical imaging: recent advances in iron- and manganese-based magnetic nanoparticles. Drug Metab Rev. 2014;46:142–54. doi:10.3109/03602532.2013.876429.
44. Nunes ADC, Ramalho LS, Souza APS, Mendes EP, Colugnati DB, Zufelato N, Sousa MH, Bakuzis AF, Castro CH. Manganese ferrite-based nanoparticles induce ex vivo, but not in vivo, cardiovascular effects. Int J Nanomed. 2014;9:3299–312.
45. Prospero AG, Quini CC, Bakuzis AF, Fidelis-de-Oliveira P, Moretto GM, Mello FPF, Calabresi MF, Matos RV, Zandoná EA, Zufelato N, et al. Real-time in vivo monitoring of magnetic nanoparticles in the bloodstream by AC biosusceptometry. J Nanobiotechnol. 2017;15:22. doi:10.1186/s12951-017-0257-6.
46. Mokgobu MI, Anderson R, Steel HC, Cholo MC, Tintinger GR, Theron AJ. Manganese promotes increased formation of hydrogen peroxide by activated human macrophages and neutrophils in vitro. Inhalation Toxicol. 2012;24:634–44. doi:10.3109/08958378.2012.706657.
47. Dorman DC, Struve MF, James RA, Marshall MW, Parkinson CU, Wong BA. Influence of particle solubility on the delivery of inhaled manganese to the rat brain: manganese sulfate and manganese tetroxide pharmacokinetics following repeated (14-day) exposure. Toxicol Appl Pharmacol. 2001;170:79–87. doi:10.1006/taap.2000.9088.
48. Park EJ, Oh SY, Lee SJ, Lee K, Kim Y, Lee BS, Kim JS. Chronic pulmonary accumulation of iron oxide nanoparticles induced Th1-type immune response stimulating the function of antigen-presenting cells. Environ Res. 2015;143:138–47. doi:10.1016/j.envres.2015.09.030.
49. Aschner M, Erikson KM, Herrero Hernandez E, Tjalkens R. Manganese and its role in Parkinson’s disease: from transport to neuropathology. Neuromol Med. 2009;11:252–66. doi:10.1007/s12017-009-8083-0.
50. Moschos SA, Bramwell VW, Somavarapu S, Alpar HO. Adjuvant synergy: the effects of nasal coadministration of adjuvants. Immunol Cell Biol. 2004;82:628–37. doi:10.1111/j.0818-9641.2004.01280.x.
51. Tran KK, Shen H. The role of phagosomal pH on the size-dependent efficiency of cross-presentation by dendritic cells. Biomaterials. 2009;30:1356–62. doi:10.1016/j.biomaterials.2008.11.034.
52. Lin PL, Flynn JL. CD8 T cells and Mycobacterium tuberculosis infection. Semin Immunopathol. 2015;37:239–49. doi:10.1007/s00281-015-0490-8.
53. Ekkens MJ, Shedlock DJ, Jung E, Troy A, Pearce EL, Shen H, Pearce EJ. Th1 and Th2 cells help CD8 T-cell responses. Infect Immun. 2007;75:2291–6. doi:10.1128/IAI.01328-06.
54. Tamburini BA, Burchill MA, Kedl RM. Antigen capture and archiving by lymphatic endothelial cells following vaccination or viral infection. Nat Communications. 2014;5:3989. doi:10.1038/ncomms4989.
55. de Paula Oliveira Santos B, Trentini MM, Machado RB, Rubia Nunes Celes M, Kipnis A, Petrovsky N, Junqueira-Kipnis AP. Advax4 delta inulin combination adjuvant together with ECMX, a fusion construct of three protective mTB antigens, induces a potent Th1 immune response and protects mice against Mycobacterium tuberculosis

infection. Hum Vaccin Immunother. 2017;13(12):2967–76. doi:10.1080/21645515.2017.1368598.
56. Comoy EE, Capron A, Thyphronitis G. In vivo induction of type 1 and 2 immune responses against protein antigens. Int Immunol. 1997;9:523–31. doi:10.1093/intimm/9.4.523.
57. Zenaro E, Donini M, Dusi S. Induction of Th1/Th17 immune response by Mycobacterium tuberculosis: role of dectin-1, Mannose Receptor, and DC-SIGN. J Leukoc Biol. 2009;86:1393–401. doi:10.1189/jlb.0409242.
58. Grosse S, Stenvik J, Nilsen AM. Iron oxide nanoparticles modulate lipopolysaccharide-induced inflammatory responses in primary human monocytes. Int J Nanomed. 2016;11:4625–42. doi:10.2147/IJN.S113425.
59. Taylor LE, Swerdfeger AL, Eslick GD. Vaccines are not associated with autism: an evidence-based meta-analysis of case-control and cohort studies. Vaccine. 2014;32:3623–9. doi:10.1016/j.vaccine.2014.04.085.
60. Price CS, Thompson WW, Goodson B, Weintraub ES, Croen LA, Hinrichsen VL, Marcy M, Robertson A, Eriksen E, Lewis E, et al. Prenatal and infant exposure to thimerosal from vaccines and immunoglobulins and risk of autism. Pediatrics. 2010;126:656–64. doi:10.1542/peds.2010-0309.
61. Blanco E, Shen H, Ferrari M. Principles of nanoparticle design for overcoming biological barriers to drug delivery. Nat Biotechnol. 2015;33:941–51. doi:10.1038/nbt.3330.
62. Weissleder R, Nahrendorf M, Pittet MJ. Imaging macrophages with nanoparticles. Nat Mater. 2014;13:125–38. doi:10.1038/nmat3780.
63. Southern P, Pankhurst QA. Commentary on the clinical and preclinical dosage limits of interstitially administered magnetic fluids for therapeutic hyperthermia based on current practice and efficacy models. Int J Hyperther. 2017;1–16. doi:10.1080/02656736.2017.1365953.
64. Mazuel F, Espinosa A, Luciani N, Reffay M, Le Borgne R, Motte L, Desboeufs K, Michel A, Pellegrino T, Lalatonne Y, et al. Massive intracellular biodegradation of iron oxide nanoparticles evidenced magnetically at single-endosome and tissue levels. ACS Nano. 2016;10:7627–38. doi:10.1021/acsnano.6b02876.
65. Gabbasov R, Cherepanov V, Chuev M, Polikarpov M, Nikitin M, Deyev S, Panchenko V. Biodegradation of Magnetic Nanoparticles in Mouse Liver From Combined Analysis of Mössbauer and Magnetization Data. IEEE Trans. Magn. 2012;49:394–7. doi:10.1109/TMAG.2012.2226148.
66. Lopez Y, Yero D, Falero-Diaz G, Olivares N, Sarmiento ME, Sifontes S, Solis RL, Barrios JA, Aguilar D, Hernández-Pando R, et al. Induction of a protective response with an IgA monoclonal antibody against Mycobacterium tuberculosis 16kDa protein in a model of progressive pulmonary infection. Int J Med Microbiol. 2009;299:447–52. doi:10.1016/j.ijmm.2008.10.007.
67. Hamasur B, Haile M, Pawlowski A, Schroder U, Kallenius G, Svenson SB. A mycobacterial lipoarabinomannan specific monoclonal antibody and its F(ab') fragment prolong survival of mice infected with Mycobacterium tuberculosis. Clin Exp Immunol. 2004;138:30–8. doi:10.1111/j.1365-2249.2004.02593.x.
68. Achkar JM, Chan J, Casadevall A. B cells and antibodies in the defense against Mycobacterium tuberculosis infection. Immunol Rev. 2015;264:167–81. doi:10.1111/imr.12276.
69. Kumar S, Anselmo AC, Banerjee A, Zakrewsky M, Mitragotri S. Shape and size-dependent immune response to antigen-carrying nanoparticles. J Control Release. 2015;220:141–8. doi:10.1016/j.jconrel.2015.09.069.
70. Fromen CA, Robbins GR, Shen TW, Kai MP, Ting JP, DeSimone JM. Controlled analysis of nanoparticle charge on mucosal and systemic antibody responses following pulmonary immunization. Proc Natl Acad Sci U S A. 2015;112:488–93. doi:10.1073/pnas.1422923112.
71. Turner DL, Bickham KL, Thome JJ, Kim CY, D'Ovidio F, Wherry EJ, et al. Lung niches for the generation and maintenance of tissue-resident memory T cells. Mucosal Immunol. 2014;7:501–10. doi:10.1038/mi.2013.67.
72. Cardona PJ, Cooper A, Luquin M, Ariza A, Filipo F, Orme IM, et al. The intravenous model of murine tuberculosis is less pathogenic than the aerogenic model owing to a more rapid induction of systemic immunity. Scand J Immunol. 1999;49:362–6. doi:10.1046/j.1365-3083.1999.00522.x.
73. Yang YK, Burkhard P. Encapsulation of gold nanoparticles into self-assembling protein nanoparticles. J Nanobiotechnol. 2012;10:42. doi:10.1186/1477-3155-10-42.
74. Schneider CA, Rasband WS, Eliceiri KW. NIH Image to ImageJ: 25 years of image analysis. Nat Methods. 2012;9:671–5. doi:10.1038/nmeth.2089.
75. Monopoli MP, Aberg C, Salvati A, Dawson KA. Biomolecular coronas provide the biological identity of nanosized materials. Nat Nanotechnol. 2012;7:779–86. doi:10.1038/nnano.2012.207.